Rivista Italiana di Paleontologia e Stratigrafia
(*Research in Paleontology and Stratigraphy*)
vol. 128(2): 539-557. **July 2022**
DOI: https://doi.org/10.54103/2039-4942/15607

GOING DEEPER INTO MODERN AND FOSSIL CROCODILIAN TOOTH MICROANATOMY: WHAT CAN BE INFERRED OF PALAEOENVIRONMENT AND TAPHONOMY FROM HISTOCHEMICAL ANALYSES?

JULIA AUDIJE-GIL[1,2,*], MARÍA CANILLAS[3], FERNANDO BARROSO-BARCENILLA[2,4], MÉLANI BERROCAL-CASERO[2,4], ADOLFO DEL CAMPO[3], ARMANDO GONZÁLEZ MARTÍN[1], JUDIT MOLERA[5], ORIOL VALLCORBA[6], MIGUEL A. RODRÍGUEZ[3] & OSCAR CAMBRA-MOO[1]

[1]Laboratorio de Poblaciones del Pasado (LAPP), Departamento de Biología, Facultad de Ciencias, Universidad Autónoma de Madrid, Madrid, 28049, Spain. E-mail: julia.audije@estudiante.uam.es; armando.gonzalez@uam.es; oscar.cambra@uam.es
[2]Grupo Paleontología Ibérica (PaleoIbérica), Departamento de Geología, Geografía y Medio Ambiente, Universidad de Alcalá, Alcalá de Henares, Madrid, 28805, Spain. E-mail: julia.audije@uah.es; fbarroso@uah.es
[3]Instituto de Cerámica y Vidrio, Consejo Superior de Investigaciones Científicas (CSIC), Madrid, 28049, Spain.
E-mail: mcanillas@icv.csic.es; adelcampo@icv.csic.es; mar@icv.csic.es
[4]Grupo Procesos Bióticos Mesozoicos, Departamento de Geodinámica, Estratigrafía y Paleontología, Universidad Complutense de Madrid, Madrid, 28040, Spain. E-mail: fbarroso@geo.ucm.es; melani.berrocal@ucm.es
[5]MECAMAT, Campus Torre dels Frares, Universitat de Vic - Universitat Central de Catalunya, Vic, 08500, Spain. E-mail: judit.molera@uvic.cat
[6]ALBA Synchrotron Light Source, Cerdanyola del Vallès, Barcelona, 08290, Spain. E-mail: ovallcorba@cells.es
*Corresponding author.

Associate Editor: Silvio Renesto.

To cite this article: Audije-Gil J., Canillas M., Barroso-Barcenilla F., Berrocal-Casero M., del Campo A., González Martín A., Molera J., Vallcorba O., Rodríguez M.A & Cambra-Moo O. (2022) - Going deeper into modern and fossil crocodilian tooth microanatomy: what can be inferred of palaeoenvironment and taphonomy from histochemical analyses? *Riv. It. Paleontol. Strat.,* 128(2): 539-557.

Keywords: *Crocodylus niloticus;* Crocodylomorph; Cretaceous; Lo Hueco; Biomineralized tissue; Hydroxyapatite.

Abstract. Teeth provide information about the evolutionary pathway of an organism, its biology and habitat. This is the case even of fossilized teeth, since they have perdurable biomineralized structures, as biological apatite. The material that has been selected for this study comprises teeth from modern crocodilian individuals and extinct Cretaceous crocodylomorphs from Lo Hueco site. Microanatomy, histochemistry and crystallographic nature of enamel, dentine and cementum have been characterized by Polarized Light Microscopy, SEM-EDS, Confocal Raman Spectroscopy and SR-µXRD. A focus has been made on dentine lamination. In the fossil sample short-period incremental lines show alternate presence of dentinal tubules that has not been described previously either in living or fossil archosaur. This could be related to influence of environmental circadian rhythms in the abundance, size and/or activity of cells depositing dentine in the day-night cycle. Regarding histochemical and crystallographic compositions, the major and mostly unique phase is HA, but in the case of fossil teeth, a secondary phase identified as hematite appears locally between discontinuities of the material. Incremental lines would not be related to variation in chemical composition and furthermore do not present different HA crystallographic nature (different directions of HA or different crystallite sizes) either. Only small intensity oscillations are observed in the fossil sample by SR-µXRD which are compatible with the alternating abundance of dentinal tubules. Crystallinity differences between modern and fossil material, as crystallite size and presence of CO_3^{2-} groups could be explained by postdepositional processes.

Received: May 20, 2021; accepted: March 15, 2022

Introduction

Teeth provide information about the evolutionary pathway of an organism and its biology and ecology (e.g., Erickson 1992, 1996; Dean 1998, 2000; Botha 2004; Dauphin & Williams 2007, 2008; García & Zurriaguz 2016; and references herein). They have perdurable biomineralized structures because of their inorganic compounds, such as biological apatite, including exceptionally well-preserved fossil teeth with microscopic cell details observable. In those fossil materials, palaeobiology and fossilization processes can be inferred, enriching palaeoenvironmental reconstruction. Study of tooth microanatomy and chemical composition allows to understand cyclical and non-cyclical events related to life history traits of individuals. This is especially relevant in organisms that maintain a close relation of dependence with the environment, such as crocodiles.

Living crocodiles have a simple dentition, compared to other extant tetrapods, which consist of conical teeth with a long root, located in alveoli (sockets: Fruchard 2012). However, crocodiles can be considered to have a pseudoheterodont pattern (Kieser et al. 1993; Thomadakis 2015) or "incipient heterodonty" (Fruchard 2012). Another important feature of crocodilian dentition is that they undergo continuous replacement of their teeth in all regions of the maxilla and jawbone (Thomadakis 2015), a condition known as polyphyodonty. Replacement is necessary to assure that the morphology of the tooth is maintained over time, with each successional tooth larger than its predecessor (Poole 1961; Thomadakis 2015), and to maintain a functional dentition throughout life.

Despite all the studies concerning dentition of extant and extinct crocodilians, there is little literature on the detailed histology and histochemistry of modern and fossil crocodilian teeth (Westergaard & Ferguson 1986, 1987; Dauphin 1987; Erickson 1992, 1996; Dauphin & Williams 2008; Fruchard 2012; Enax et al. 2013; Gren & Lindgren 2014; Thomadakis 2015). The three dental tissues, enamel, dentine and cementum, differ in microanatomy, microstructure and chemical composition (Hillson 2005), as well as their two interphases (enamel-dentine junction, EDJ, and cementum-dentine junction, CDJ). The chemical composition may vary in the distribution of some elements, but the main phase is constituted by a biological apatite of nanometric structure, the hydroxyapatite (HA; Hurlbut & Klein 1982). When a tooth grows and erupts dentine fills the pulp cavity until it occludes it, leaving a record of odontogenesis (Erickson 1992, 1996). This record is observed in all the tissue typologies of the teeth, but precisely in the dentine, different incremental lines and bands are identified (Erickson 1992, 1996; Dean 1998, 2000). On the one hand, short-period incremental lines of von Ebner (1906; described for the first time by Owen 1845) are a thin lamination that represents circadian increments in dentine formation rate. While ultradian or infradian rhythm (periodicity of less than a day) in dentine and enamel have been documented as well (Dean & Scandrett 1996; Dean 1998). Short-period incremental lines are identified as dark and light lines of varying widths (around 20-μm average). Chemical labelling has determined the daily rhythm in the accumulation and mineralization of dentine in crocodylians (Erickson 1992, 1996). Moreover, these daily increments are a shared primitive character in amniotes and they are considered a homology in Mesozoic crocodylomorphs and non-avian dinosaurs. On the other hand, long-period incremental lines of Andresen (1898) contain a variable number of short-period incremental lines (so they are wider bands), representing more than one day of accumulation and mineralization of dentine. They are supposed to depend partially on endogenous biorhythms (Dean & Scandrett 1996). Nevertheless, in crocodilian teeth odontogenesis the environment also has influence in the dentine deposit, taking into account that warm cycles and seasons are favourable for biological apatite synthesis (Domingo et al. 2015).

To understand the cyclicity of events, novel techniques of palaeohistological and physicochemical analysis have been employed here in modern and fossil crocodilian teeth. The aim of this work is to carry out a comparative characterization of biological and taphonomical features in terms of microanatomy and micropreservation events, to discern if features in the inner structure are the result of the growth kinetics or of taphonomical origin.

Geological setting of the fossil sample

Lo Hueco is an Upper Cretaceous palaeontological site in "Garumn" facies located in the locality of Fuentes (Cuenca, Central-Eastern Spain) discovered and excavated in 2007 (Barroso-

Barcenilla et al. 2009). The stratigraphic position and the palaeontological content allow assignment to the upper Campanian-lower Maastrichtian. Concerning geological information, among the levels and structures of the site, four beds contain vertebrate remains and have been proposed as four different taphofacies (Cambra-Moo et al. 2012a): the sandy channel structure (C), two grey marly mudstone levels (G1 and G2) and one red marly mudstone level (R2). This site is interpreted as a near coastal marsh and muddy flood plain with sandy channels with input from brackish to fresh water sources (Barroso-Barcenilla et al. 2009). Levels G1 and G2 represent the proximal and distal part of the flooded muddy plain and they contain the majority of the best-preserved fossils of the site.

Concerning palaeontological information, more than 10,000 macroremains have been recovered in Lo Hueco, mainly belonging to vertebrates, but also to plants and invertebrates. Its rich and varied fossil assemblage is considered as one of the most important vertebrate collections in the whole European record of the Upper Cretaceous. Among crocodylomorphs, Lo Hueco have provided a great number of articulated and isolated cranial and postcranial elements. All these crocodylomorph remains probably belong to at least two groups of non-Crocodylia eusuchians, close to allodaposuchids (Ortega et al. 2015). Allodaposuchidae are grouped beside Hylaeochampsidae in the sister group of Crocodylia, the only crocodyliform lineage alive today and to which it belongs *Crododylus niloticus*. At a preservational level, Lo Hueco has been proposed as a Concentration Lagerstätte because of its density of remains and diversity of taxa (Cambra-Moo et al. 2012a). Moreover, the exceptional quality of tissues preservation demonstrates that Lo Hueco exhibits areas of exceptional preservational potential (Cambra-Moo et al. 2012a; 2013). A first taphonomical approach by Cambra-Moo et al. (2012a) identified patterns and events that allows unveiling biostratinomic and fossil diagenetic processes, which are more deeply analysed, in the present work.

Materials and methods

Materials

The material that has been selected for this study comprises 8 teeth (4 of modern crocodilians and 4 of fossil crocodylomorphs). The 4 modern teeth (KD1, KD2, KD4 and KD5; Fig. 1A) belong to individuals in different ontogenetic stages (from juveniles to early adult stage; Audije-Gil et al. in press.) of the African species *Crocodylus niloticus* Laurenti, 1768. This material was donated by the crocodile farm Granja de Cocodrilos Kariba (Jerez de la Frontera, Southern Spain). The 4 fossil teeth (G1-C-177, G1-C-288, G2-O-200 and G2-W-016; Fig. 1B) belong to unknown allodaposuchids from the Upper Cretaceous site of Lo Hueco (Fuentes, Central-Eastern Spain). Teeth come from two different stratigraphic levels of grey marly mudstone level: G1 and G2.

Methods

All the teeth were measured and photographed prior to the preparation of thin sections. The modern teeth thin sections were prepared at the Instituto de la Cerámica y Vidrio (ICV-CSIC, Madrid, Spain) following the methodology proposed by Cambra-Moo et al. (2012b, 2014). The fossil teeth thin sections were prepared at the Laboratorio de Preparación de Láminas Delgadas of the Departamento de Geodinámica, Estratigrafía y Paleontología of the Universidad Complutense de Madrid (Spain). In all samples the procedure was similar with slightly modifications due to the properties presented by different materials. Each tooth was embedded in a mixture of transparent resin and catalyst, under vacuum, to fill all the teeth cavities with the mixture. A 1 to 3-millimeter-thick longitudinal section was obtained from each tooth, from the base to the mid-crown apex, with a circular diamond slow-speed saw. Then, they were fixed on petrographic slides with a mounting adhesive and manually polished to approximately 100-micron-thickness (to obtain optical translucency). This procedure was carried out using different grits of silicon carbide (SiC) sandpaper and powder, in the modern and fossil sample respectively. Subsequently, samples were studied and analysed by mean of Polarized Light Microscopy (PLM) at the Laboratorio de Poblaciones del Pasado (LAPP) of the Universidad Autónoma de Madrid (Spain); by Scanning Electron Microscopy-Energy Dispersive X-ray spectroscopy (SEM-EDS) and Confocal Raman Spectroscopy at the ICV-CSIC (Madrid, Spain); and by Synchrotron-radiation X-ray micro-diffraction (SR-μXRD) at the ALBA synchrotron of Cerdanyola del Vallès (Barcelona, Spain).

Polarized Light Microscopy (PLM). General palaeohistological features of the different tissue typologies of all thin sections from modern and fossil teeth (Fig. 1C-F) were observed using a linearly polarized light microscope (CX31, Olympus Corporation, Tokyo, Japan). Thin sections were sequentially imaged at 5× magnification with a 10.0MP digital USB camera (A35100U, OMAX Corporation, Kent, USA) associated to the microscope and the imaging software ToupView Driver 2.0 (Hangzhou ToupTek Photonics Co., Zhejiang, China). Then a complete high-resolution photomontage was edited using Photoshop CC 2014 software (Adobe Systems Incorporated, San José, USA). The digital calibrated ruler of ToupView Driver 2.0 was used on the images when measurements were necessary.

Scanning Electron Microscopy-Energy Dispersive X-ray spectroscopy (SEM-EDS). Five teeth were selected for the subsequent histochemical analyses by SEM-EDS and following techniques, to determine the identity of their mineral phases. They were the modern crocodilian teeth KD1 and KD4, and the fossil crocodylomorph teeth G1-C-177, G2-O-200 and G2-W-016. Samples were coated with a thin layer of Silver (Ag), operating at 20 kV of accelerating voltage and 12-14 mm of working distance. Subsequently submicron scale structures and elemental composition of the five teeth were characterized with cold cathode field emission scanning electron microscope FESEM S-4700 (Hitachi, Tokyo, Japan).

Confocal Raman Spectroscopy (Raman). A deeper level of the chemical composition and crystallinity of the dental tissues was analysed with a Confocal Raman microscope ALPHA 300AR (WITec, Ulm, Germany) equipped with a Nd:YAG laser light source (532 nm). The microscopy setup was mounted in a piezo-driven scan plat-

form having 4 nm lateral and 0.5 nm vertical positioning accuracy. Raman images of different sizes were recorded in backscattering configuration through a 100× objective with a numerical aperture of 0.95 and an integration time of 1 s per pixel. Optical resolution was of approximately 300 nm in the longitudinal direction and 500 nm in transversal direction. To facilitate the analysis of micro-Raman spectroscopical analysis, the background was subtracted by adjusting it to a polynomial of order 9, due mainly to fluorescence emission. The sample could be measured with sufficient intensity at 10 mW, except in the case of areas with iron oxide with a hematite structure (considered in the results as a postdepositional artefact) where power should be reduced. Raman mappings were taken in XY in different areas and were analysed by using Witec Project Plus Software.

Synchrotron-radiation X-ray micro-diffraction (SR-μXRD). In order to characterize teeth hydroxyapatite (HA) crystalline structure, three teeth (modern KD1, and fossil G2-O-200 and G1-C-177) were analysed by SR-μXRD technique at the ALBA synchrotron BL04 Materials Science and Powder Diffraction (MSPD) beamline (Fauth et al., 2013). To carry this out, additional transversal 500 μm thickness sections were prepared. The areas of interest from the polished thin sections samples were measured in transmission geometry with a focused beam of 15×15 μm^2 (full width at half-maximum). The energy used was 29.2 keV (λ = 0.4246 Å) and the diffraction patterns were recorded with a Rayonix SX165 CCD detector (active area of 165 mm diameter, frame size 2048×2048 pixels, 79 μm pixel size, dynamic range 16 bit) positioned at 245 mm of the samples. Diffraction patterns were collected along lines traced in radial directions from the outside to the inner areas of the teeth, with a periodicity of 10 μm. Instrumental calibration (from NIST- 660b LaB6 data collected in the same conditions) and conversion of the 2D XRD images to powder diffraction patterns have been performed with software (Vallcorba & Rius 2019).

Results

Macroscopically, the modern and fossil teeth do not present evident postdepositional alterations, mostly superficial that not implicate changes in the normal tooth anatomy, so all samples could be considered as well-preserved (Fig. 1A-B).

Polarized Light Microscopy (PLM; Fig. 1C-M)

Microscopically, all the modern and fossil teeth present an exceptional preservation of their tissues microanatomy (Fig. 1C-F). Concerning modern crocodilian sample, in KD1 and KD2 enamel exhibits a rough contour because this tissue was apparently still in formation. Moreover, there is a lamination in enamel parallel to the profile of the teeth, with more or less equidistant incremental lines of about 10-40 μm (Fig. 1G). Dentine also shows this type of equidistant incremental lines, alternating dark and light intervals and of about 10-40 μm too (Fig. 1I); and wider light-dark bands that contain a variable number of shorter incremental lines. In the case of cementum (Fig. 1K), wide bands of about 50-100 μm thickness are observed. In the two smaller modern teeth, KD4 and KD5, the enamel, dentine and cementum are identified, but they did not present incremental lamination probably due to the biostratinomic processes that altered their microanatomy (Fig. 1D).

Regarding the fossil crocodylomorph sample, none of the teeth exhibit enamel lamination lamination (Fig. 1H). In addition, enamel shows some microcracks and it is largely absent from some areas (especially in G1-C-177 and G2-O-200) where dentine is directly exposed to the surface. As previously described in the modern sample, two sort of incremental lines are identified in the dentine structure. The short-depositional periods are of about 10-40 μm (Fig. 1J); and the long-depositional ones present again variable thickness. A ferruginous material precipitated between some layers and inside porosity (infilling through microcracks; Fig. 1L). Part of the

Fig. 1 - Macroscopical and microscopical view (in Polarized Light Microscopy) of the modern (left column) and fossil (right column) crocodilian teeth. A) Modern sample, three views (anterior, right lateral and posterior) per tooth. B) Fossil sample, three views (anterior, right lateral and posterior) per tooth. C-D) Thin section photomontage of modern teeth KD1 (C) and KD4 (D). KD1 shows a replacement tooth inside still in formation without root (and consequently, without cementum) that presents enamel and dentine with their corresponding incremental lines. E-F) Thin section photomontage of fossil tooth G1-C-177 (E) and G2-W-016 (F). G) Detail of enamel in modern tooth KD1, where lamination parallel to the profile of the EDJ can be observed (yellow arrows). H) Detail of enamel in fossil tooth G2-W-016, where enamel prisms arrangement can be observed. I) Dentine in modern tooth KD1, with short-period incremental lines (yellow arrows) and clear-dark intervals representing long-period incremental bands of variable widths (among white arrows). J) Dentine in fossil tooth G1-C-177, with short-period incremental lines (yellow arrows) and clear-dark intervals representing long-period incremental bands of variable widths (among white arrows). Ferruginous material can be observed between some layers and inside porosity. K) Cementum in modern tooth KD1. L) Microfracture (black arrow) in enamel of fossil tooth G2-W-016, through which ferruginous material has infilled. M) Cementum in fossil tooth G2-W-016, partially replaced by ferruginous material. Abbreviations: CDJ = Cementum-dentine junction; CE = Cementum; DE = Dentine; EDJ = Enamel-dentine Junction; EN = Enamel. Scale bars from A-F = 1 mm; scale bars from G-M = 100 μm.

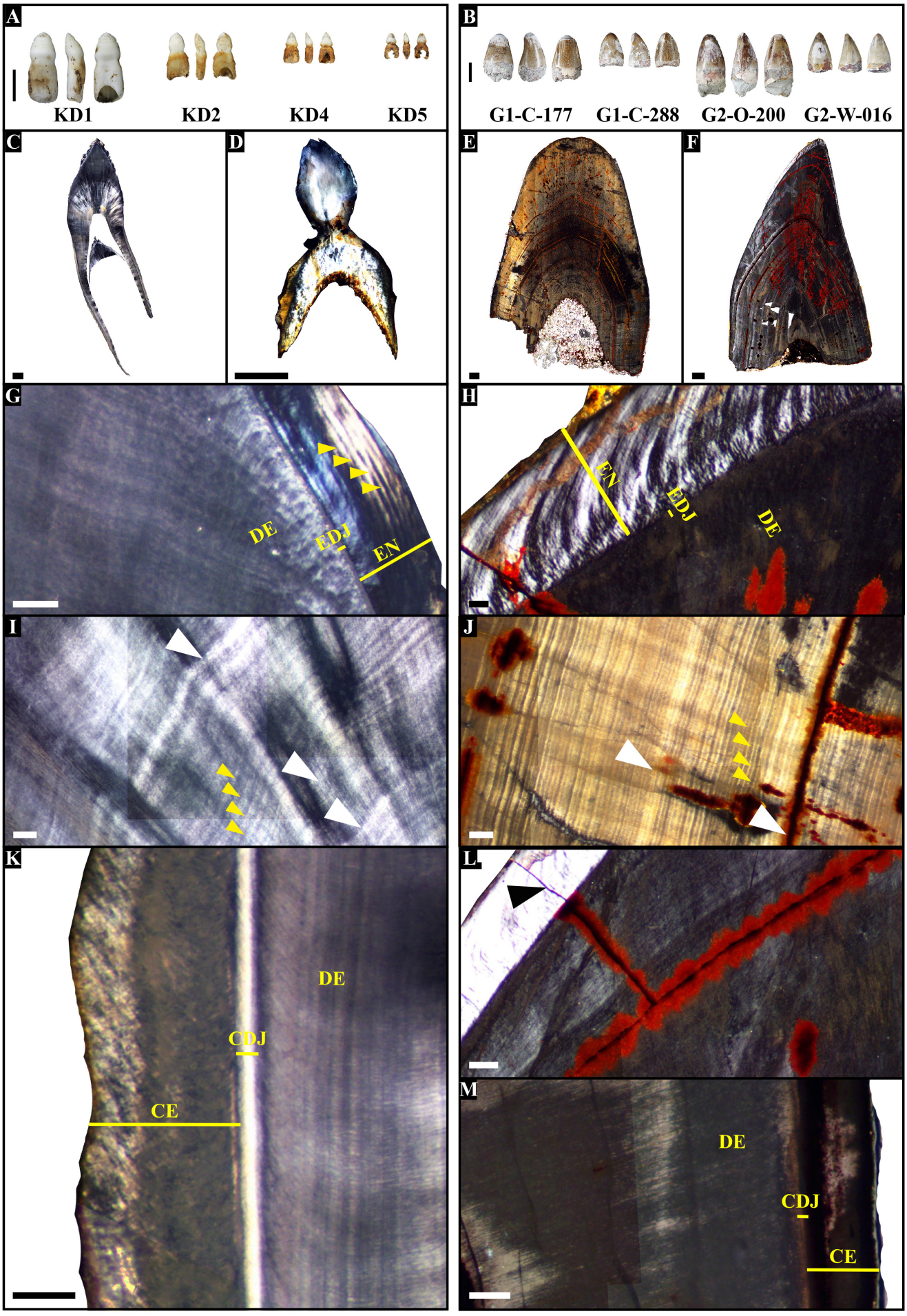
A
KD1
KD2
KD4
KD5
B
G1-C-177
G1-C-288
G2-O-200
G2-W-016
C
D
E
F
G
DE
EDJ
EN
H
EN
EDJ
DE
I
J
K
DE
CDJ
CE
L
M
DE
CDJ
CE

root cementum is preserved in the fossil specimens in a remnant of the root neck and it is significantly altered (Fig. 1M). In most areas, this tissue is completely replaced by ferruginous material, where a lamination of 10-40 μm can be observed.

Scanning Electron Microscopy-Energy Dispersive X-ray spectroscopy (SEM-EDS; Fig. 2A-F)

In modern teeth, enamel incremental lines (Fig. 2A) do not present differences in their elemental chemical composition. These teeth have a Calcium/Phosphorus (Ca/P) ratio around 1.67 (coincident with the composition of biological apatite) in enamel and dentine. However, dentine is less mineralized (i.e. Ca/P ratio remains similar but counts of both elements decrease). This slight mineralization change (Fig. 2C) occurs in the interphase region of about 20 μm, identified as the enamel-dentine junction (EDJ). The EDJ shows minor differences with respect to the dentine Ca/P ratio, although it is a more porous area in comparison to the crown and root dentine. In the dentine of the modern teeth, no lamination is observed by SEM and there are not notable differences in the Ca/P ratio in the sampled areas. At higher magnification, some cavities of approximately 1 μm diameter are observed. These are distributed regularly and they are identified as the porosity generated by the odontocytes cytoplasmic extensions (or dentinal tubules; Fig. 2E). Magnesium (Mg) presence in the dentine is scarce and constant, showing no differential distribution associated to lamination. With regard to cementum, it appears as a very porous tissue with large cavities and without lamination (Fig. 2I). A similar Ca/P ratio is observed in cementum and root dentine, but this ratio is higher than expected in biological apatite. Nevertheless, dentine is less mineralized, decreasing from the interphase, the cementum-dentine junction (CDJ; Fig. 2G).

Unlike the modern sample, no periodic lamination is observed in the enamel of the fossil teeth (Fig. 2B). Enamel and dentine present the same Ca/P ratio, with the enamel in some areas less mineralized (Fig. 2D). Besides, in fossil teeth the EDJ is less mineralized than both enamel and dentine. Iron (Fe) presence of postdepositional origin is detected inside this layer in G1-C-177. Regarding dentine, the analysis of the micrometric texture reveals two undulation levels. These surface unevenness on the mineral phase are identified as incremental lines. In many areas of the fossil sample there is a relation between those short-period lines and the distribution of the dentinal tubules. Alternate lines of more porosity (greater presence of dentinal tubules) and less porosity (smaller presence of dentinal tubules) are observed (Fig. 2F). In other areas, the dentinal tubules are distributed regularly. There is no important variation in the composition of each short-period line in fossil teeth (i.e., there are not significant changes in the Ca/P ratio along the same line and nor between different lines: Fig. 2H). There are either no differences in composition between different points of the long-period lines. Moreover, in the fossil sample, the values of the Ca/P ratio of the dentine are higher than expected for the biological apatite, especially in most altered areas. In addition, Iron (Fe) is present in zones of discontinuity. This Fe does not have a biological origin, as it penetrated through the postdepositional microcracks discontinuities between layers and porosity.

Fig. 2 - Main Scanning Electron Microscopy-Energy Dispersive X-ray spectroscopy (SEM-EDS) high-resolution images and main graphic results of the modern (left column) and fossil (right column) crocodilian teeth. A) Detail of apex enamel of modern tooth KD1, with consecutive incremental lines (yellow arrows) presented as undulations in the surface. B) Lateral enamel in fossil tooth G1-C-177, with several microfractures and without lamination. C) Mineralization change between enamel and dentine in modern tooth KD4. D) Mineralization change between enamel and dentine in fossil tooth G2-W-016. E) Dentine in modern tooth KD4, where no type of lamination can be observed. Cavities of 1 μm and regularly distributed correspond to dentinal tubules. F) Alternative lines of greater porosity (greater presence of dentinal tubules) and less porosity (less presence of dentinal tubules) in dentine of fossil tooth G2-W-016. On the left, three short-period incremental lines (yellow arrows) with one of the areas with less dentinal tubules highlighted by dashed yellow lines. On the right, magnification of one region with less porosity highlighted by dashed white lines. Scale bar corresponds to right image. G) Mineralization change between cementum and dentine in modern tooth KD4. H) Calcium/Phosphorus (Ca/P) ratio in 3 short-period lines in fossil tooth G2-W-016, where it can be observed that the ratio is constant, despite the fact that Ca and P counts go up and down due to lines topography and discontinuities. I) Detail of modern tooth KD4 cementum, with large cavities. J) Detail of fossil tooth G2-W-016 cementum with similar appearance to modern cement, despite taphonomical alteration and microfractures. Abbreviations: CDJ = Cementum-dentine junction; CE = Cementum; DE = Dentine; EDJ = Enamel-dentine Junction; EN = Enamel.

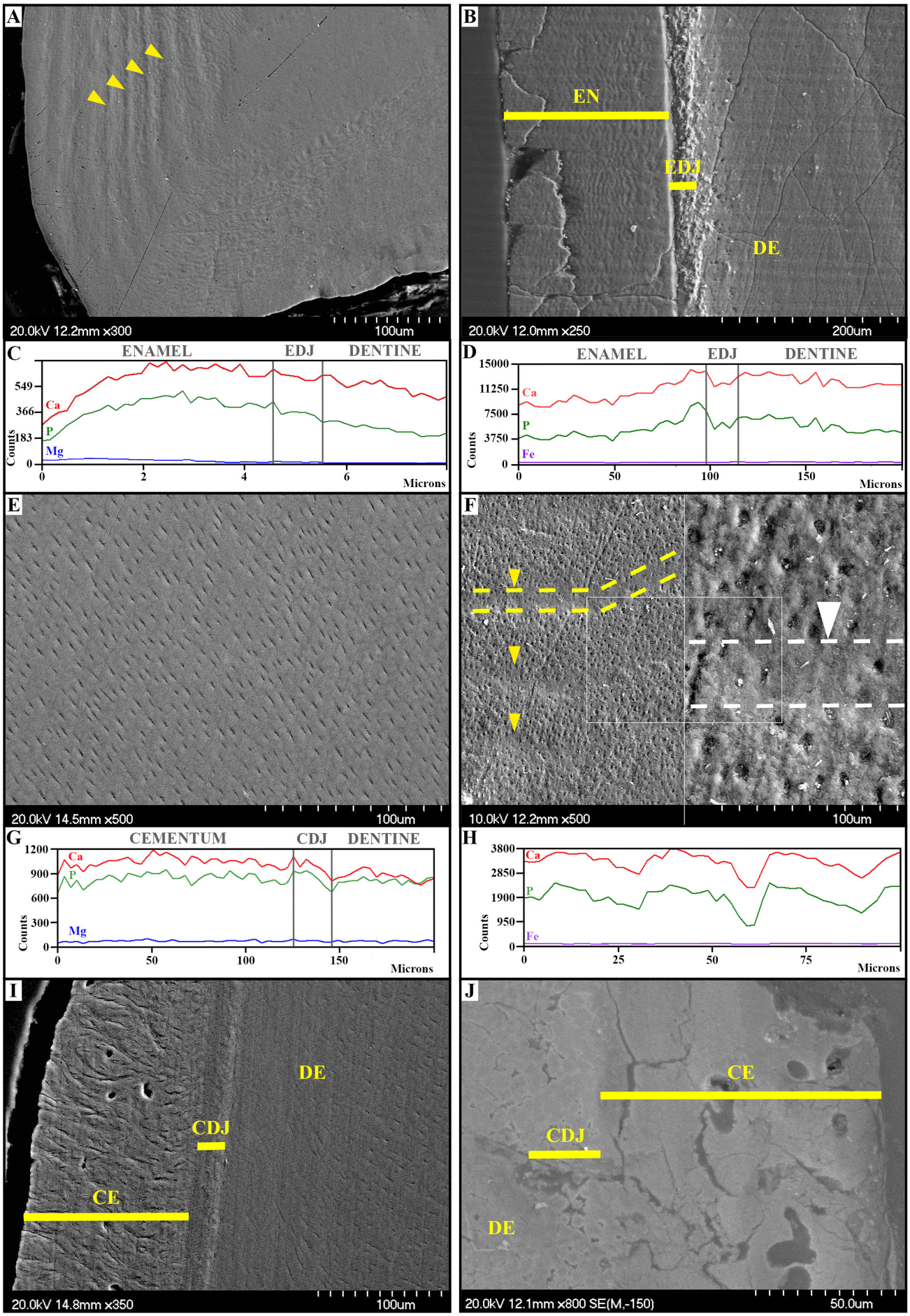
A
20.0kV 12.2mm x300
100um
B
EN
EDJ
DE
20.0kV 12.0mm x250
200um
C
ENAMEL
EDJ
DENTINE
549
366
183
0
Ca
P
Mg
Counts
0
2
4
6
Microns
D
ENAMEL
EDJ
DENTINE
15000
11250
7500
3750
0
Ca
P
Fe
Counts
0
50
100
150
Microns
E
20.0kV 14.5mm x500
100um
F
10.0kV 12.2mm x500
100um
G
CEMENTUM
CDJ
DENTINE
1200
900
600
300
0
Ca
P
Mg
Counts
0
50
100
150
Microns
H
3800
2850
1900
950
0
Ca
P
Fe
Counts
0
25
50
75
Microns
I
DE
CDJ
CE
20.0kV 14.8mm x350
100um
J
CE
CDJ
DE
20.0kV 12.1mm x800 SE(M,-150)
50.0um

The Ca/P ratio sharply decreases when there is presence of Fe, due to the substitution of the biological apatite by the ferruginous material. In G2-W-016, there is presence of small amounts of Sulphur (S) as well as abundant Fe close to those microcracks and other areas that present postdepositional alteration. The presence of Mg has not been observed in any of the sampled areas of the fossil teeth. High resolution images of cementum show a very porous tissue with large cavities from biological origin and microcracks originated by postdepositional processes (Fig. 2J). Its Ca/P ratio is similar to that of dentine. Moreover, in fossil cementum, elemental analyses reveal the presence of Silicon (Si) and Aluminium (Al), both from postdepositional origin related to the presence of clays in the sediment.

Confocal Raman Spectroscopy (Raman; Fig. 3A-D)

The typical bands of hydroxyapatite (HA) vibration modes are found in all sample, being the ν1 of HA phosphate (PO_4^{3-}) group the main and most intense band. It appears around 960 cm^{-1}. Three more bands with lower intensities are found around 430, 580 and 1040 cm^{-1}. They correspond to ν2, ν3 and ν4 vibration modes of PO_4^{3-} group of HA. However, some differences are observed between the spectra of different zones and different teeth. Concerning modern remains, in enamel, the band at 960 cm^{-1} is slightly displaced towards lower Raman shifts with respect to dentine (Fig. 3A). Besides, the intensity of 1071 cm^{-1} band is higher than in dentine. This band is associated to ν1 of carbonate (CO_3^{2-}) in B type carbonated HA, where CO_3^{2-} are substituting PO_4^{3-} groups. In crown and root dentine, the results show again the most intense band at 960 cm^{-1}. In addition, the band at 1071 cm^{-1} appears although its intensity is lower than in the enamel. As in SEM-EDS elemental results, the short and long-period incremental lines do not present any difference in the Raman spectra. In the dentinal tubules, there is a wide band at 296 cm^{-1} and a narrower at 568 cm^{-1}. Both are not found elsewhere in the dentine and could be associated to changes in HA crystals orientation. The root dentine band at 1071 cm^{-1} is weak (Fig. 3B), with HA having less carbonate in this area. Moreover, in root dentine there is a higher concentration of dentinal tubules than in the crown, but there are no differences on both regions from the Raman spectroscopy point of view. In the CDJ and in the cementum there is a band at 960 cm^{-1} that is less symmetric and wider (i.e., less ordered or with smaller crystallite size) than in enamel and dentine. In general, HA is slightly displaced 0.3 cm^{-1} at lower Raman shift in the cementum (Fig. 3B centre) compared to other tissues and it presents an intense band at 1071 cm^{-1} (Fig. 3B right). The intensity of this band is higher in enamel and cementum than in dentine, which indicates a greater presence of CO_3^{2-} groups in these regions. Whereas, the cementum HA is more similar to the crown and root dentine than to enamel. In the modern sample, three additional bands appear in the spectra of dentine and cementum but not in enamel. These bands at 816, 855 and 1004 cm^{-1} correspond to proline, hydroxiproline and phenylalanine (Morris & Mandair 2011), which are amino acids involved in the cellular activity.

Concerning fossil remains, enamel presents a HA spectrum with intense fluorescence (Fig. 3C). Nevertheless, the band at 960 cm^{-1} of HA can be

Fig. 3 - Main Confocal Raman Spectroscopy results of the modern (above) and fossil (below) crocodilian teeth. A) Above, image in confocal microscopy of enamel in modern tooth KD1, with detail map in one area, and graphical results with average spectra of XY mappings in enamel and two areas of the dentine. Below, image in confocal microscopy of dentine in the same tooth, with detail map in one area (in red hydroxyapatite, in blue dentinal tubules), and histogram of Raman shift in enamel and two areas of dentine. B) Image in confocal microscopy of cementum in modern tooth KD1, with detail map of Raman shift of 960 cm^{-1} band around interphase cementum-dentine, and graphical results with average spectra of XY mappings in enamel, root dentine and cementum. C) Image in confocal microscopy of enamel in fossil tooth G2-W-016, with detail map of Raman shift of 960 cm^{-1} band around interphase enamel-dentine, and graphical results with average spectra of XY mappings in enamel and dentine. D) Above, image in confocal microscopy of dentine in fossil tooth G2-W-016, with detail map in three areas (in red HA, in blue dentinal tubules), and graphical results with average spectra of XY mappings in those three areas in dentine. Below, image in confocal microscopy of microcrack in the same tooth, filled with hematite in dentine (in red HA, in green hematite filling microcrack and adjacent dentinal tubules), and graphical results with average spectra of XY mappings in two areas of dentine.
Abbreviations: CDJ = Cementum-dentine junction; CE = Cementum; DE = Dentine; EDJ = Enamel-dentine Junction; EN = Enamel. Black scale bars = 100 μm; white scale bars = 5 μm.

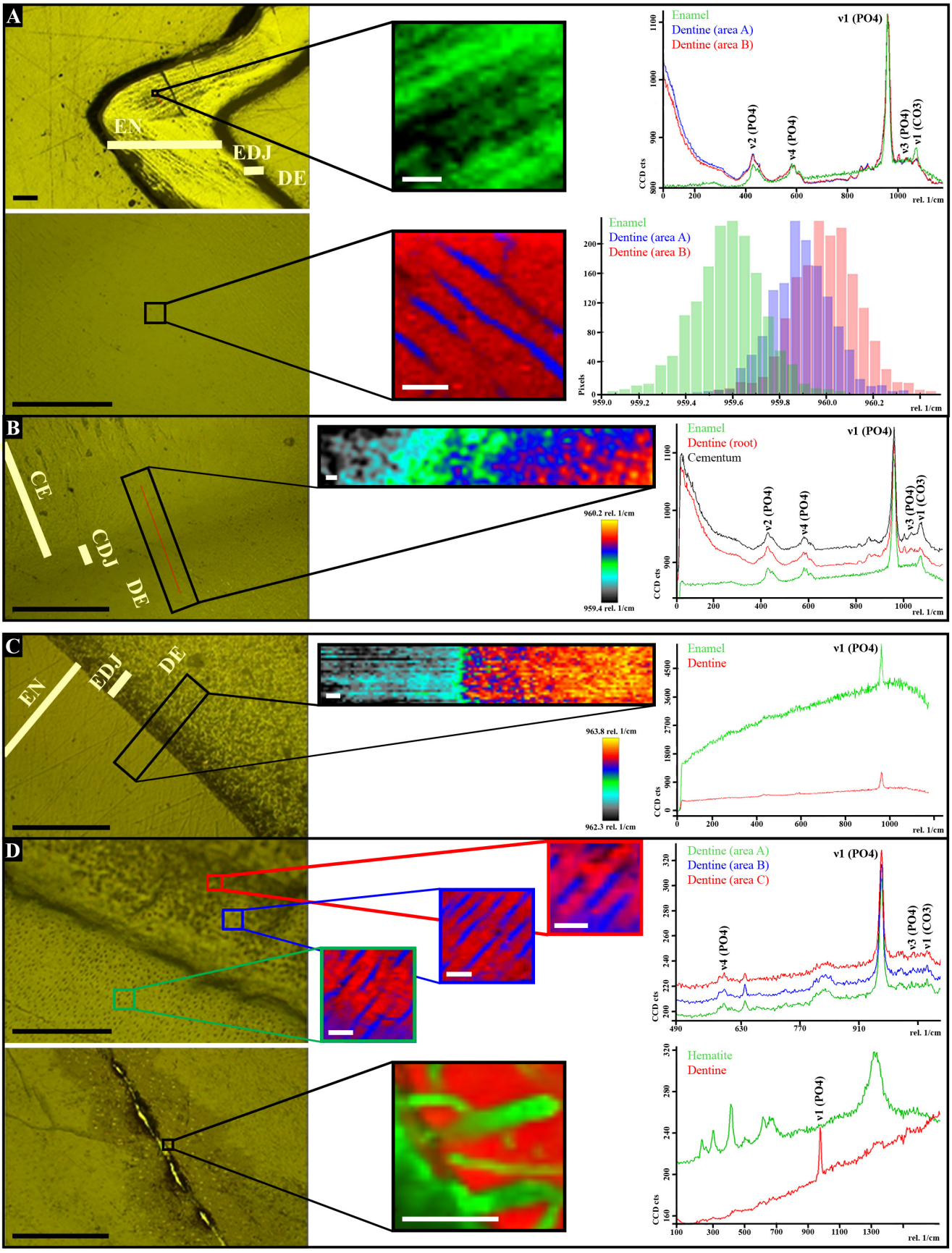
A
EN
EDJ
DE
Enamel
Dentine (area A)
Dentine (area B)
v1 (PO4)
v2 (PO4)
v4 (PO4)
v3 (PO4)
v1 (CO3)
CCD cts
rel. 1/cm
Pixels
B
CE
CDJ
DE
Enamel
Dentine (root)
Cementum
960.2 rel. 1/cm
959.4 rel. 1/cm
C
EN
EDJ
DE
Enamel
Dentine
963.8 rel. 1/cm
962.3 rel. 1/cm
D
Dentine (area A)
Dentine (area B)
Dentine (area C)
Hematite
Dentine

observed, appearing displaced at lower Raman shift than in the modern sample. On the contrary, in the dentine that band is always displaced around 3 cm^{-1} at higher Raman shifts (i.e. ν1 for PO_4^{3-} groups between 962 to 963 cm^{-1}) compared to the modern sample. The ν1 of CO_3^{2-} is observed in dentine of the fossil teeth although it does not have much intensity (Fig. 3D). In this tissue, there are two chemical phases. The main phase is HA, with expected bands at 961 cm^{-1} for ν1, and 430 and 580 cm^{-1} for ν2 and ν3 vibration modes. Short-period lines can be observed in dentine under confocal Raman microscopy as a series of dark and light lines, but there is no Raman spectra difference between them. The darker lines show greater presence of dentinal tubules than the clearer ones. In general, dentinal tubules show slight degree of carbonation in their Raman spectra with respect to dentine, and some are empty or filled with embedding resin. In the fossil cementum, as in the enamel, the band of HA is always displaced more than 1 cm^{-1} towards lower Raman shifts with respect to dentine, showing that cementum is less crystalline material. Finally, the spectra of the second phase reveals an Iron oxide (Fe_2O_3), corresponding to hematite, that leaked through growth lines and the adjacent porosity. These results fully coincide with those obtained by SEM-EDS.

Synchrotron-radiation X-ray micro-diffraction (SR-μXRD; Fig. 4A-F)

The use of SR-μXRD helps to clarify deep crystalline differences between the main crystalline phase (HA) in enamel and dentine of modern and fossil teeth. Diffraction patterns show significant differences regarding the peak width, especially in the dentine, with much better defined peaks in the case of fossil teeth (Fig. 4A). In modern material, no significant variations of the diffraction patterns can be observed, but in the case of fossil material, notable structural changes are found when entering the inner surface of the tooth (Fig. 4C). From the tooth external surface down to 400-500 μm depth (comprising the enamel and some of the dentine), the HA crystals are highly oriented with the c-axis perpendicular to the EDJ surface. Then, the HA orientation becomes completely random and an abrupt displacement of some diffraction peaks to higher angles can be observed, corresponding to a reduction of the lattice parameter (Fig. 4B). The c parameter experiments a slight expansion down to the 400-500 μm depth but in much less amount. The cell parameters remain constant in further inner zones of the dentine, where only the increase of the peak widths can be observed. This increase of widths leads to the complete overlapping of the main diffraction peaks of HA, the (211) and (112) planes. When a data collection scan has been made through the areas containing Fe, according to the SEM-EDS analysis, new diffraction peaks assigned to the hematite phase have been identified (Fig. 4D). The spatial distribution of hematite in depth indicates that the inclusions in discontinuities of the material are of about 30 μm.

Regarding the dentine lamination, in all cases the diffraction patterns were taken every 10 μm along lines entering to the teeth. In this sense, no crystallographic variations are observed along the incremental lines of the modern and fossil teeth. Patterns in areas further inside the dentine corresponding to a 60 μm zone (6 patterns) are shown in Fig. 4E. A close inspection of the intensities from the main peaks exhibits small variations. The intensity of the peaks corresponding to planes

Fig. 4 - Main Synchrotron-radiation X-ray micro-diffraction (SR-μXRD) results of the modern and fossil crocodilian teeth. A) Powder diffraction pattern of the dentine in modern KD1 and fossil G1-C-177 teeth, at 900-micron depth, with the reflection indices of hydroxyapatite (HA) main peaks. A 3000 counts intensity offset has been applied to the fossil tooth data for clarity. B) Evolution of the lattice parameters of HA crystal structure in depth in the fossil tooth G1-C-177. C) Stacking of the powder diffraction patterns along a measurement line from the outside to the inside of the fossil tooth G1-C-177 (100 points spaced by 10 μm between them), through the enamel (blue) and the dentine (black) zones. The red patterns correspond to a zone in the dentine where the HA crystals loose the orientation and experiment a strong reduction of its *a* lattice parameter. A 2D XRD image is shown for each of the HA states, oriented and non-oriented. D) Stacking of diffraction patterns along a 100 μm zone (10 patterns) with the assignment of the hematite phase peaks identified by Confocal Raman Spectroscopy. The spatial distribution of hematite infilling along a 1000 μm zone for the fossil tooth G2-O-200 according to the intensity of the (012) peak is shown. E) Stacking of powder diffraction patterns through a 60 mm scan (6 patterns) in the fossil tooth G1-C-177, where small intensity variations can be observed on the HA diffraction peaks. F) Variation of the intensity of (211+112) and (300) HA diffraction peaks in depth in the fossil tooth G1-C-177.

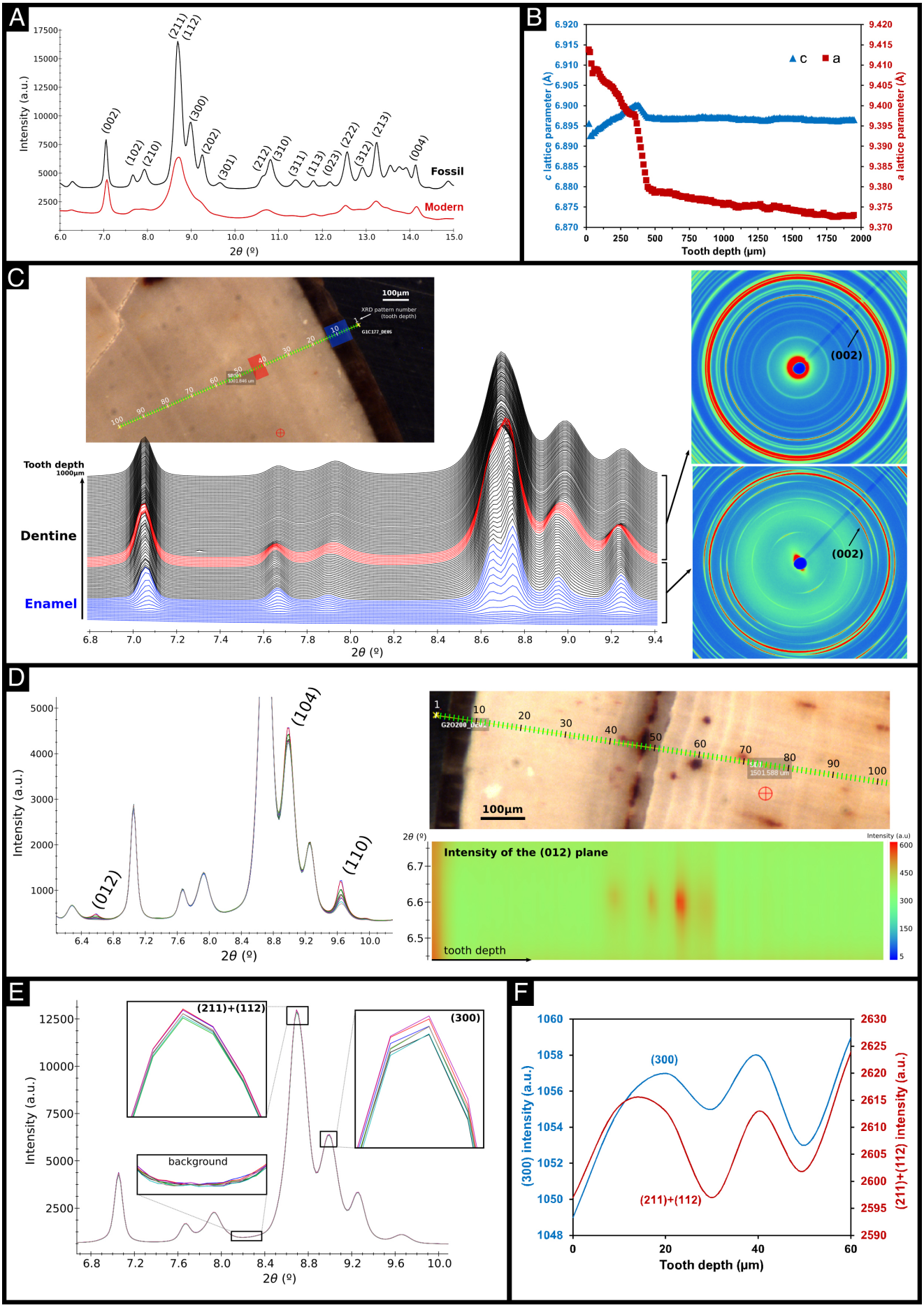
A
Intensity (a.u.)
2θ (º)
(002)
(102)
(210)
(211)
(112)
(300)
(202)
(301)
(212)
(310)
(311)
(113)
(023)
(222)
(312)
(213)
(004)
Fossil
Modern
B
c lattice parameter (Å)
a lattice parameter (Å)
c
a
Tooth depth (µm)
C
100µm
XRD pattern number (tooth depth)
Tooth depth
1000µm
Dentine
Enamel
2θ (º)
(002)
(002)
D
Intensity (a.u.)
(012)
(104)
(110)
2θ (º)
100µm
Intensity of the (012) plane
tooth depth
E
Intensity (a.u.)
(211)+(112)
(300)
background
2θ (º)
F
(300) intensity (a.u.)
(211)+(112) intensity (a.u.)
(300)
(211)+(112)
Tooth depth (µm)

(211)+(112) (totally overlapping) and (300) follows a sequence (Fig. 4F) with a distance equal to that between the incremental lines. This could be explained by the presence of differential porosities in these laminations, which causes less material to diffract and therefore changes in the intensity of diffraction. The fact that there is no changes in the position or in the relative intensities of the peaks indicates the absence of a different crystallographic nature between the different incremental lines and bands.

Discussion

The analysis of modern crocodilian and fossil crocodylomorph teeth using high-resolution techniques have provided two possible ways of inference. The first one allows for describe main histochemical features inside the same sample (modern or fossil) by deepening in microanatomy, microstructure and chemical characterization down to the crystallographic level; the second one allows for comparison between modern and fossil material and their changes along time. Instead of doing separate analyses by each way of inference, they have been considered rather complementary since by deepening in microanatomy it is possible to discern if features in the inner structure are the result of the growth kinetics or from taphonomical origin. Main results of the present work and ways of inference are summarized in Suppl. tab. 1.

Starting with Polarized Light Microscopy (PLM) and Scanning Electron Microscopy (SEM; two first results columns of Suppl. tab. 1), these techniques have been applied to study microanatomy and microstructure of enamel, dentine and cementum. Enamel (light and dark green in Suppl. tab. 1) in extant and extinct crocodilians is thin, around 100-200 μm (Enax et al. 2013), being thicker at the crown apex and finer towards the limit with the root (Figs. 1C-H, 2A-B). This is accordant with crocodilian teeth function since these reptiles use teeth to grab and secure the prey with the jaw before swallowing (Grigg & Kirshner 2015), but not to cut or chew, which are much more abrasive habits. Comparing enamel microanatomy of modern and fossil teeth by PLM and SEM, it has been observed that there is an absence of lamination in the latter. Enamel incremental lamination has been previously described in mammals (Dean 2000; and references therein) but poorly reported in non-mammalian tetrapods (Dauphin 1987; O'Meara et al. 2018). However, its absence in the fossil sample would not be related to a biological difference but rather to postdepositional microevents, as discussed below. Unlike enamel, which is an acellular tissue with scarce porosity, cementum (light and dark blue in Suppl. tab. 1) is the most porous material of both samples and has the greatest cavities for the cellular component of the tooth and this causes that cementum to be the most altered tissue where sediment has infilled. Incremental lamination in cementum, here observed in both samples, has been proposed as the result of seasonal changes in mammals (Lieberman 1993).

Regarding microanatomy and microstructure of dentine (light and dark brown in Suppl. tab. 1), which is the most abundant tissue in the tooth, short and long-period incremental lines previously described in the literature (e.g. Erickson 1992, 1996; Dean 1998, 2000) have been identified here by PLM. In both samples, the lamination is more irregular and diffuse near the apex, while it is more regular close to the pulp cavity. This is because as the tooth erupts, dentine is gradually deposited towards the pulp cavity (Poole 1961), and because the apex is most subject to biomechanical pressures (Erickson et al. 2012; Vallcorba et al. 2021), as indicated by the crystallographic results (Fig. 4B) showing hydroxyapatite (HA) texture down to a certain tooth depth. In living amniotes, short-period lines are from 1 to 30 μm in width, independently of the tooth shape and size. This is explained by a physiological or structural limitation in the amount of dentine that can be deposited daily (Erickson 1992). The incremental lines in extinct crocodylomorphs are considered morphologically equivalent to those in extant crocodilians and thus, they are the result of a biologic process of growth and not the consequence of postdepositional changes. Comparing both samples, the fossil material shows alterations by the conditions of diagenesis and secondary mineralization, similar to that described by Gren and Lindgren (2014) that in some areas obliterate the original microanatomy but overall lamination is exceptionally preserved. Thus, it is assumed that these crocodylomorphs had a circadian rhythm of dentine deposit as it has

been observed in other amniotes (Erickson 1996).

The odontocytes are responsible for that dentine deposition and mineralization (Fruchard 2012), leaving their cytoplasmic extensions micrometric cavities, the dentinal tubules. In the modern sample, the dentinal tubules are distributed regularly (Fig. 2E) although those cavities are more abundant in the root than in the crown. However, in some areas of the fossil sample, where the lamination is best preserved, alternate short-period incremental lines with greater porosity (greater presence of dentinal tubules) and less porosity (less presence of dentinal tubules) appear (Fig. 2F). In other words, the lines that are observed at the optical level (which reflect the daily increments with a light and dark line representing a day) are also observed in the microanatomy of some parts of the fossil dentine. This alternate presence of dentinal tubules in short-period incremental lines has not been described previously either in living or fossil archosaurs, which usually present regular distribution in dentine (Dauphin & Williams 2008; Enax et al. 2013). It could be related with crocodilian development, which is very dependent of environmental conditions (Cott 1961; Revol 1995; Fruchard 2012). Although extant crocodilians show different seasonal trends in their biological cycles according to day length and temperature (Grigg & Kirshner 2015), little is known about how daily conditions affects their physiology. Some works have shown how their behaviour and habits may depend on daily rhythms (Campbell et al. 2010), which seem to be related with a melatonin source that control start and timing of events (Firth et al. 2010). However, the mechanism of daily photoperiod response and whether it is equivalent in all species remains unknown. So that, the finding of alternate presence of dentinal tubules in crocodylomorphs from Lo Hueco opens a new field of study with palaeobiological implications, as these reptiles seem to have influence of environmental circadian rhythms in the abundance, size and/or activity of cells depositing dentine in the day-night cycle. Besides that, this inference could also help in paleoenvironmental reconstructions, as seasonal changes (cooling and warming episodes) have been documented in the Campanian-Maastrichtian (Domingo et al. 2015), but there is a lack of information regarding environmental daily conditions.

Deepening in teeth structure, chemical and crystallographic compositions (three rightmost results columns of Suppl. tab. 1) have been analysed by high-resolution techniques: Scanning Electron Microscopy-Energy Dispersive X-ray spectroscopy (SEM-EDS), Confocal Raman spectroscopy (Raman) and Synchrotron-radiation X-ray microdiffraction (SR-μXRD). The main phase, HA, has been observed in enamel, dentine and cementum of both modern and fossil teeth. In the case of the fossil teeth a secondary phase identified as hematite by Raman results (Figs. 3D, 4D), appearing locally between discontinuities of the material (Fig. 1L). In previous work on the geological context and preservation at Lo Hueco site, three taphonomical phases were identified in the fossil bones of the site (Barroso-Barcenilla et al. 2009; Cambra-Moo et al. 2012a). In the first one, primary gypsum filled the natural cavities and microcracks of most vertebrate remains of Lo Hueco (Carenas et al. 2011). In the second phase, a ferruginous material covered the surface of most of the remains and filled some of the inner cavities (Barroso-Barcenilla et al. 2009; Cambra-Moo et al. 2012a). This material corresponds with the hematite phase and its formation took place after organic matter decay, in early diagenetic process, and in alkaline conditions of shallow burials (Bao et al. 1998). In the third and final phase, a precipitation of secondary gypsum occurred, reaching also internal cavities in most of vertebrate remains (Carenas et al. 2011). Although gypsum is very abundant in Lo Hueco, it is not present in the inner cavities of the fossil teeth. Postdepositional macroevents induced infiltration and penetration of mineral-charger water in the larger cavities of the biomineralized tissues (as vascular canals and osteons in bones) and subsequent precipitation of gypsum, hematite and again, gypsum. Nevertheless, these minerals differentially precipitated into the smaller cavities, as dentinal tubules, where the presence of the ferruginous phase has been found, but not sulphate. This may be related to the size of the dentinal tubules (micron scale) and that they correspond to hermetic isolate or rarely connected cavities rather than to a communicated system. This is in accordance with the fact that most dentinal tubules are empty in the fossil teeth and only those near discontinuities of the lamination and microcracks produced in early diagenetic phase are infilled of hematite.

Focusing on chemical and crystallographic characterization of the main phase (HA), Raman results in the modern material shows differences in the intensity of the band associated to ν1 of carbonate (CO_3^{2-}) between tissue typologies and samples. The carbonate presence is related to the substitution of hydroxyl (OH^-) and phosphate (PO_4^{3-}) groups (Okada & Matsumoto 2015) by CO_3^{2-} group in B type carbonated HA, destroying the symmetry of the HA (Penel et al. 1998). Biological apatite is a non-stoichiometric form of HA where the most common substituting ion is CO_3^{2-}. Raman spectroscopy results show that there is a large presence of CO_3^{2-} in the modern sample of this work (Figs. 3A-B), which is in accordance with the fact that crocodylian teeth are constituted by a carbonated HA (Enax et al. 2013). In relation to this, the larger diffraction peak width observed by SR-μXRD (Fig. 4A) indicates a smaller crystallite size in modern teeth compared to the fossil remains, which is usual in the case of carbonated HA (Calasans-Maia et al. 2015). Carbonated HA presence may be quite high during early tissue mineralization (Shah et al. 2016). So that, this seem to be the case since analysed modern teeth belongs to young or early adult stage individuals (Audije-Gil et al., in press.). This would explain why external tissues (enamel and cementum), which are the last to form, have a higher content of that CO_3^{2-} groups. Comparing modern and fossil material, the fossil teeth the crystallinity is higher (larger crystallite size) than in the modern and the slight presence of CO_3^{2-} was identified by Raman spectroscopy but not by SR-μXRD. This latter is probably due to its presence in a very small quantity. The smaller amount of CO_3^{2-} groups could be due to usual carbonate disappearance during fossilization process. In Lo Hueco there is no carbonated exoskeleton of invertebrates, there are only clayey moulds (Barroso-Barcenilla et al. 2009; Cambra-Moo et al. 2012a). Moreover, it is known that HA crystallites subjected to high temperature (which is usually involved in diagenesis) lose CO_3^{2-} groups. The eliminated CO_3^{2-} from the HA structure release energy that increase crystallite size (Fernández-Jalvo et al. 2018; Grupe 2018). However, it is also possible that different crystallite sizes between modern and fossil teeth could be due to different metabolism in extant and extinct individuals, the latter having slower growth and thus, depositing larger crystallites.

To add information concerning second way of inference (Suppl. tab. 1), chemical and crystallographic characterization of HA phase in the three tissue typologies separately have been analysed. SEM-EDS results in the modern sample show that enamel has a higher amount of Ca and P than dentine, which corresponds to a HA with higher mineral content. Although there is a greater amount of these elements in the sampled enamel of this work (Fig. 2C), the difference with respect to dentine is not as marked as expected (Dauphin & Williams 2008; Enax et al. 2013). In the case of the fossil sample, enamel has even less mineral content than dentine in some areas (Fig. 2D) and furthermore, there is no presence of lamination. Enamel HA crystallites are larger than those of dentine (Carlson 1989) and they compound the tissue with less organic matter (i.e., less porosity). This should apparently make it less prone to degradation (Domingo et al. 2015; Grupe 2018). Nevertheless, enamel acellular characteristic makes it less flexible and thus, more prone to microcracks and diagenetic alteration, as demineralization and recrystallization (Grupe 2018). Because of that, enamel in fossil teeth presents a HA spectrum with much more fluorescence than in dentine (Fig. 3C; Fernández-Jalvo et al. 2018). Moreover, enamel and cementum are the most exposed tissues to the sediment and the most probably altered by postdepositional processes.

Concerning dentine in both samples, the short and long-period incremental lines have been traditionally considered as the consequence of variation in collagen fibres trajectory (i.e., different direction of dentine deposit; Erickson 1996; Hillson 2005) or/and changes in the ratio of the mineral phase and the organic material (Dauphin & Williams 2008). In addition, in works carried out in other extant crocodilian species, as *Crocodylus porosus* (Dauphin & Williams 2008; Enax et al. 2013), a high Mg content has been reported in dentine. Dauphin and Williams (2008) observed differences in chemical distribution of Mg, Ca and P, which were associated to incremental lines. However, the results of the present work show that lamination do not seem to be related with changes in chemical composition as there are not significant changes in the Ca/P ratio along the same line and nor between different ones (Figs. 2G-H). Moreover, in either modern or fossil sample, the presence of Mg is

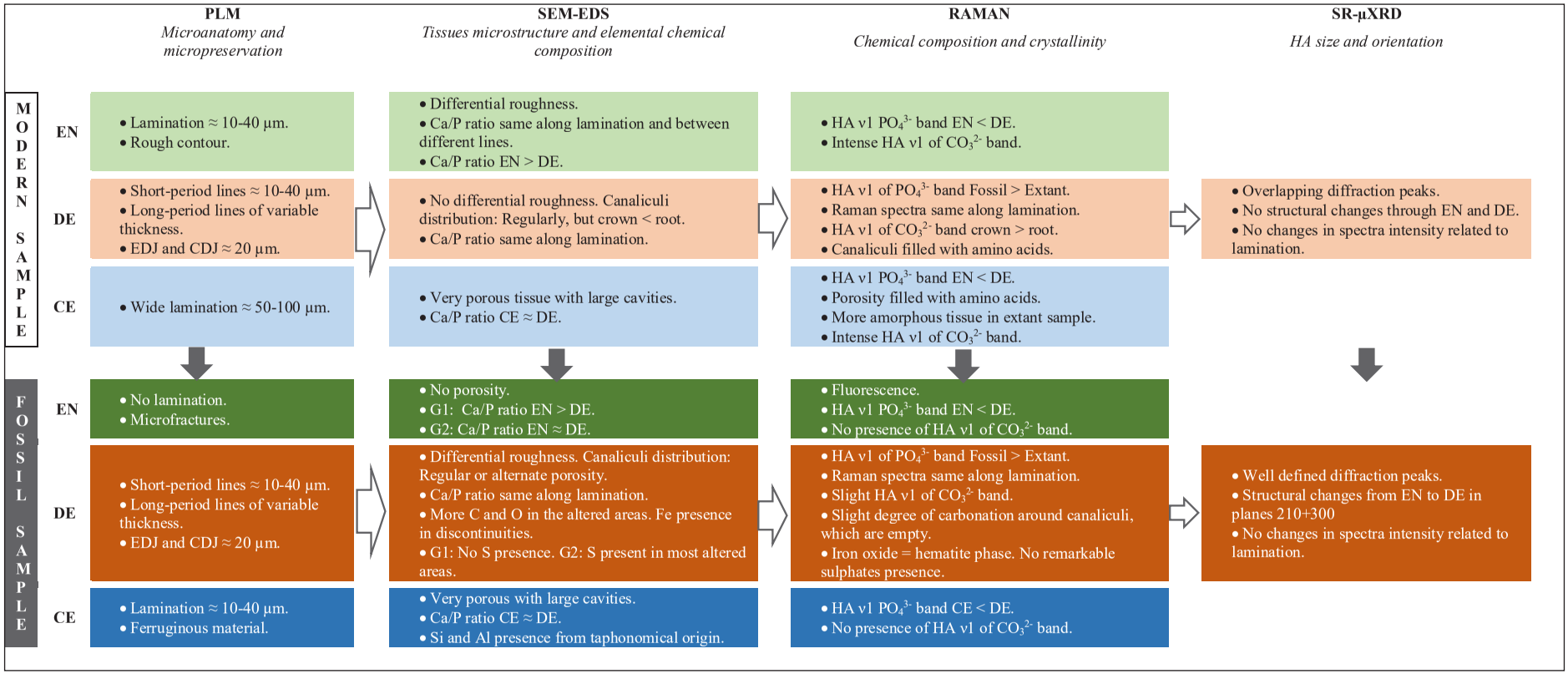

Suppl. Tab. 1 - Summary of main results by Polarized Light Microscopy (PLM), Scanning Electron Microscopy-Energy Dispersive X-ray spectroscopy (SEM-EDS) and Confocal Raman spectroscopy (Raman) and Synchrotron-radiation X-ray micro-diffraction (SR-µXRD) in enamel (EN; light and dark green), dentine (DE; light and dark brown) and cementum (CE; light and dark blue) of modern and fossil crocodilian teeth. Grey empty arrows indicating deepening in microanatomy, microstructure and chemical characterization down to the crystallographic level; and grey filled arrows indicating changes over time in relation to biological and postdepositional events. Abbreviations: Al = Aluminium; C = Carbon; Ca/P = Calcium/Phosphorus; CO32- = Carbonate; CDJ = Cementum-dentine junction; EDJ = Enamel-dentine Junction; G1 = Level G1 of Lo Hueco site: G2 = Level G2 of Lo Hueco site; HA = Hydroxyapatite; O = Oxygen; PO43- = Phosphate; Si = Silicon.

anecdotic and not variable between incremental lines. Although this require further study, it could be related to the fact that *C. porosus* lives in estuaries with brackish or saltwater (Grigg & Kirshner 2015), where Mg concentration is higher than in fresh water. Therefore, these crocodiles acquire higher amount of Mg in the diet and by water diffusion (Grigg 1981), so their electrolyte concentration physiological fluids is different than exclusive freshwater species. This would indicate that physiology of crocodylomorphs from Lo Hueco should be more like freshwater crocodiles, as *C. niloticus*, than marine species, and despite having brackish influence they show preferential ingestion of freshwater (Domingo et al. 2015).

Furthermore, short and long-period incremental lines do not seem to be related in the studied sample with different HA crystallographic nature either. Small intensity oscillations are observed in the fossil teeth by SR-μXRD but they are compatible with the alternating abundance of dentinal tubules (Fig. 4F). Regarding structural changes, they have been observed only in the case of the fossil material towards the interior of the teeth. There is a strong orientation of the HA crystals in the enamel, the enamel-dentine junction (EDJ) and a region of the dentine. Then, in the dentine there seems to be a transition zone, at about ~450 μm in depth, where the HA orientation disappears and it is the lattice parameter which experiments an abrupt reduction, while the c parameter remains rather constant (Fig. 4B). This matches with some colour changes in the teeth section (long-period lines) as previously reported by Vallcorba et al. (2021). In this sense, differences in HA orientation may be due to metabolic cycles and the influence in tooth microanatomy of changes in the environment, since fossil specimens where more subject to unstable environmental conditions than modern specimen from a farm, were environment (temperature, food supply, etc.) is controlled and homogeneous. Nevertheless, a more in-depth study with higher spatial resolution becomes necessary to try to clarify optical differences observed along lamination in both modern and fossil material are the result of two different deposition directions of the HA during dentine formation; or the presence of different HA crystallite sizes (i.e. different deposition speeds, fast or slow) depending on cell abundance, size and/or activity.

Conclusions

The comparative study of microanatomy and microstructure of the three tissue typologies (enamel, dentine and cementum) in modern and fossil crocodilian teeth shows that the most exposed tissues, enamel and cementum, are the most altered by postdepositional processes. Enamel in the modern sample present a lamination, which is probably the result of seasonal changes, that is missing in the fossil material due to recrystallization processes. Dentine deposition in modern and fossil sample presents lamination in the form of long and short-period incremental lines. In the fossil sample, short-period lines deposition suggest a circadian rhythm and reveal two alternative presence of dentinal tubules in daily incremental lines that have not been observed in modern taxa (whose lamination is regular) nor previously described in literature. This differential porosity coinciding with short-period incremental lines probably implies greater/lower abundance, size and/or activity of cells depositing dentine in the day-night cycle of Lo Hueco crocodylomorphs and thus higher influence on environmental conditions related to day-night cycles.

Regarding chemical and crystallographic characterization, the only identified majority phase, both in modern and fossil teeth, is hydroxyapatite (HA). Besides, in the case of fossil teeth, hematite appears locally infilling discontinuities of the material produced during fossilization mechanical pressures in the weakening regions of the teeth. Concerning the main phase, HA, crystallinity in enamel and dentine is lower in the modern teeth than in the fossil and the presence of CO_3^{2-} has not been identified by SR-μXRD in fossil material probably to its low content. Crocodylian teeth are constituted by a carbonated hydroxyapatite so that, the low presence of CO_3^{2-} groups could be due to partial release during diagenesis. The eliminated CO_3^{2-} from the structure produce free energy that increase HA crystallite size. However, it is possible that different metabolism in extant and extinct individuals.

Dentine short and long-period incremental lines do not show significant changes in Ca and P presence along the same line and nor between different ones. Moreover, in either modern or fossil sample, the presence of Mg is anecdotic and not associated to lamination. This latter, would indicate that way of life and physiology of crocody-

lomorphs from Lo Hueco should be more like *C. niloticus* than saltwater species as *C. porosus*. With all that, incremental lines would not be related to variation in chemical composition and furthermore do not present different HA crystallographic nature (different directions of HA or different crystallite sizes) either. Only small intensity oscillations are observed in the fossil sample by SR-μXRD, which are compatible with the alternating abundance of dentinal tubules, due to metabolic cycles and the influence of changes in the environment.

Acknowledgments: We thank Á. Conde Alonso, director of the Granja de Cocodrilos Kariba (Jerez de la Frontera, Spain), for kindly donation of the modern *C. niloticus* material for this study. We want to recognize the work made by the reviewers and editors of this manuscript, who have contributed to its improvement with their corrections and comments. We also thank the financial support of Consejo Superior de Investigaciones Científicas (CSIC, Spain) [in the frame of projects CSIC-201760E022 and CSIC-201860E127] and Ministerio de Economía y Competitividad (Spain) [CGL2015-66604, CGL2015-68363, HAR2016-78036-P, HAR2016-74846-P, HAR2017-82755-P, HAR2017-83004-P and PGC2018-099405-B-100]. Part of the experiments were performed at the BL04 Materials Science and Powder Diffraction (MSPD) beamline of the ALBA Synchrotron [proposal ALBA-2019023466].

References

Andresen V. (1898) - Die Querstreifung des Dentines. *Deutsche Monatsschrift für Zahnheilkunde*, 38: 386-9.

Audije-Gil J., Barroso-Barcenilla F. & Cambra-Moo O. (in press) - Mapping histovariability and growth patterns of Crocodylus niloticus bred in captivity and its paleobiological implications. In: Farlow J.O. & Woodward H.N. (Eds.) - Crocodylian Biology and Archosaur Paleobiology: Studies in Honor of Ruth M. Elsey. Indiana University Press, Bloomington.

Bao H., Koch P.L. & Hepple R.P. (1998) - Hematite and calcite coatings on fossil vertebrates. *Journal of Sedimentary Research*, 68(5): 727-738.

Barroso-Barcenilla F., Cambra-Moo O., Escaso F., Ortega F., Pascual A., Pérez-García A., Rodríguez-Lázaro J., Sanz J. L., Segura M. & Torices A. (2009) - New and exceptional discovery in the Upper Cretaceous of the Iberian Peninsula: the palaeontological site of "Lo Hueco", Cuenca, Spain. *Cretaceous Research*, 30(5): 1268-1278.

Botha J., Lee–Thorp J., & Sponheimer M. (2004) - An examination of Triassic cynodont tooth enamel chemistry using Fourier Transform infrared spectroscopy. *Calcified tissue international*, 74(2): 162-169.

Calasans-Maia M.D., Melo B.R.D., Alves A.T.N.N., Resende R.F.D.B., Louro R.S., Sartoretto S.C., Granjeiro J.M. & Alves G.G. (2015) - Cytocompatibility and biocompatibility of nanostructured carbonated hydroxyapatite spheres for bone repair. *Journal of Applied Oral Science*, 23(6): 599-608.

Cambra-Moo O., Barroso-Barcenilla F., Berreteaga A., Carenas B., Coruña F., Domingo L., Domingo M. S., Elvira A., Escaso F., Ortega F., Pérez-García A., Peyrot D., Sanz J. L., Segura M., Sopelana A. & Torices A. (2012a) - Preliminary taphonomic approach to "Lo Hueco" palaeontological site (Upper Cretaceous, Cuenca, Spain). *Geobios*, 45(2): 157-166.

Cambra-Moo O., Nacarino-Meneses C., Rodríguez-Barbero M.Á., García-Gil O., Rascón-Pérez J., Rello-Varona S., Campo-Martín M. & González-Martín A. (2012b) - Mapping human long bone compartmentalisation during ontogeny: A new methodological approach. *Journal of Structural Biology*, 178(3): 338-349.

Cambra-Moo O., Barroso-Barcenilla F., Coruña F. & Postigo-Mijarra J. M. (2013) - Exceptionally well-preserved vegetal remains from the Upper Cretaceous of 'Lo Hueco', Cuenca, Spain. *Lethaia*, 46(1): 127-140.

Cambra-Moo O., Nacarino-Meneses C., Rodríguez-Barbero M. Á., García-Gil O., Rascón-Pérez J., Rello-Varona S., D'Angelo M., Campo-Martín M. & González-Martín A. (2014) - An approach to the histomorphological and histochemical variations of the humerus cortical bone through human ontogeny. *Journal of anatomy*, 224(6): 634-646.

Campbell H.A., Sullivan S., Read M.A., Gordos M.A. & Franklin C.E. (2010) - Ecological and physiological determinants of dive duration in the freshwater crocodile. *Functional Ecology*, 24(1): 103-111.

Carenas B., Barroso-Barcenilla F., Berreteaga A., Cambra-Moo O., Coruña F., González-Acebrón L. & Segura M. (2011) - First overview on gypsum in the new and exceptional "Lo Hueco" fossil site (Upper Cretaceous, Cuenca, Spain). In: Sampson D. H. (Ed.) - Gypsum: Properties, Production and Applications: 176-190. Nova Publishers, New York.

Carlson S.J. (1989) - Vertebrate dental structures. In: Carter J.G. (Ed.) - Skeletal Biomineralization: Patterns, Processes and Evolutionary Trends, 235-260. *American Geophysical Union*, Washington D. C.

Cott H.B. (1961) - Scientific results of an inquiry into the ecology and economic status of the Nile crocodile (*Crocodilus niloticus*) in Uganda and Northern Rhodesia. *The transactions of the Zoological Society of London*, 29(4): 211-356.

Dauphin Y. (1987) - Implications of preparation processes on the interpretation of reptilian enamel structure. *Paläontologische Zeitschrift*, 61(3-4): 331.

Dauphin Y. & Williams C.T. (2007) - The chemical compositions of dentine and enamel from recent reptile and mammal teeth - variability in the diagenetic changes of fossil teeth. *CrystEngComm*, 9 (12): 1252-1261.

Dauphin Y. & Williams C.T. (2008) - Chemical composition of enamel and dentine in modern reptile teeth. *Mineralogical Magazine*, 72(1): 247-250.

Dean M.C. (1998) - Comparative observations on the spacing of short-period (von Ebner's) lines in dentine. *Archives of Oral Biology*, 43(12): 1009-1021.

Dean M.C. (2000) - Incremental markings in enamel and den-

tine: what they can tell us about the way teeth grow. In: Teaford M.F., Smith M.M. & Ferguson M.W. (Eds.) - Development, function and evolution of teeth: 119-130. Cambridge University Press, Cambridge.

Dean M.C. & Scandrett A.E. (1996) - The relation between long-period incremental markings in dentine and daily cross-striations in enamel in human teeth. *Archives of Oral Biology*, 41(3): 233-241.

Domingo L., Barroso-Barcenilla F. & Cambra-Moo O. (2015) - Seasonality and Paleoecology of the Late Cretaceous Multi-Taxa Vertebrate Assemblage of "Lo Hueco" (Central Eastern Spain). *PloS One*, 10(3): e0119968.

Ebner V. von (1906) - Über die Entwicklung der leimgebenden Fibrillen, insbesondere im Zahnbein. S*itzungsberichte der Mathematisch-Naturwissenschaftlichen Klasse der kaiserlichen Akademie der Wissenschaften in Wien*, 115: 281-347.

Enax J., Fabritius H.O., Rack A., Prymak O., Raabe D. & Epple M. (2013) - Characterization of crocodile teeth: correlation of composition, microstructure, and hardness. *Journal of Structural Biology*, 184 (2): 155-163.

Erickson G.M. (1992) - Verification of von Ebner incremental lines in extant and fossil archosaur dentine and tooth replacement rate assessment using counts of von Ebner lines (PhD thesis). Montana State University, 54 pp.

Erickson G.M. (1996) - Daily deposition of dentine in juvenile Alligator and assessment of tooth replacement rates using incremental line counts. *Journal of Morphology*, 228(2): 189-194.

Erickson G.M., Gignac P.M., Steppan S.J., Lappin A.K., Vliet K.A., Brueggen J.D., Inouye B.D., Kledzik D. & Webb G.J. (2012) - Insights into the ecology and evolutionary success of crocodilians revealed through bite-force and tooth-pressure experimentation. *PLoS One*, 7(3): e31781.

Fauth F., Peral I., Popescu C. & Knapp M. (2013) - The new material science powder diffraction beamline at ALBA synchrotron. *Powder Diffraction*, 28(S2): S360-S370.

Fernández-Jalvo Y., Tormo L., Andrews P. & Marin-Monfort M.D. (2018) - Taphonomy of burnt bones from Wonderwerk Cave (South Africa). *Quaternary International*, 495: 19-29.

Firth B.T., Christian K.A., Belan I. & Kennaway D.J. (2010) - Melatonin rhythms in the Australian freshwater crocodile (*Crocodylus johnstoni*): a reptile lacking a pineal complex?. *Journal of Comparative Physiology B*, 180(1): 67.

Fruchard C. (2012) - The Nile crocodile, a new model for investigating heterodonty and dental continuous renewal in vertebrates. *BioSciences Master Reviews*: 1-10.

García R.A. & Zurriaguz V. (2016) - Histology of teeth and tooth attachment in titanosaurs (Dinosauria; Sauropoda). *Cretaceous Research*, 57: 248-256.

Gren J.A. & Lindgren J. (2014) - Dental histology of mosasaurs and a marine crocodylian from the Campanian (Upper Cretaceous) of southern Sweden: incremental growth lines and dentine formation rates. *Geological Magazine*, 151(1): 134-143.

Grigg G. (1981) - Plasma homeostasis and cloacal urine composition in *Crocodylus porosus* caught along a salinity gradient. *Journal of Comparative Physiology*, 144(2): 261-270.

Grigg G. & Kirshner D. (2015) - Biology and evolution of crocodylians. Cornell University Press, Ithaca, 649 pp.

Grupe G. (2018) - Taphonomy and fossilization. The International Encyclopedia of Biological Anthropology: 1-8.

Hillson S. (2005) - Teeth. Cambridge University Press, Cambridge, 373 pp.

Hurlbut C.S. & Klein C. (1982). Manual de mineralogía de Dana. Editorial Reverté, Barcelona, 564 pp.

Kieser J.A., Klapsidis C., Law L. & Marion M. (1993) - Heterodonty and patterns of tooth replacement in *Crocodylus niloticus*. *Journal of Morphology*, 218(2): 195-201.

Laurenti J.N. (1768). Specimen medicum: exhibens synopsin reptilium emendatam cum experimentis circa venena et antidota reptilium austriacorum. Joan Thomae, Viena.

Lieberman D.E. (1993) - Life history variables preserved in dental cementum microstructure. *Science*, 261(5125): 1162-1164.

Morris M.D. & Mandair G.S. (2011) - Raman assessment of bone quality. *Clinical Orthopaedics and Related Research*, 469(8): 2160-2169.

Okada M. & Matsumoto T. (2015) - Synthesis and modification of apatite nanoparticles for use in dental and medical applications. *Japanese Dental Science Revien,* 51(4): 85-95.

O'Meara R.N., Dirks W. & Martinelli A.G. (2018) - Enamel formation and growth in non-mammalian cynodonts. *Royal Society Open Science*, 5(5): 172293.

Ortega F., Cambra-Moo O., Mocho P., Vidal D. & Sanz J.L. (2015) - The biota of the Upper Cretaceous site of Lo Hueco (Cuenca, Spain). *Journal of Iberian Geology*, 57: 591-623.

Owen R. (1845) - Odontography, or, a treatise on the comparative anatomy of the teeth, their physiological relations, mode of developement, and microscipic structure, in the vertebrate animals. Hippolyte Bailliere, London, 655 pp.

Penel G., Leroy G., Rey C. & Bres E. (1998) - MicroRaman spectral study of the PO_4 and CO_3 vibrational modes in synthetic and biological apatites. *Calcified tissue international,* 63(6): 475-481.

Poole D.F.G. (1961) - Notes on tooth replacement in the Nile crocodile *Crocodilus niloticus*. *Proceedings of the Zoological Society of London*, 136 (1): 131-140.

Revol B. (1995) - Crocodile farming and conservation, the example of Zimbabwe. *Biodiversity and Conservation*, 4(3): 299-305.

Shah F.A., Snis A., Matic A., Thomsen P. & Palmquist A. (2016) - 3D printed Ti6Al4V implant surface promotes bone maturation and retains a higher density of less aged osteocytes at the bone-implant interface. *Acta biomaterialia*, 30: 357-367.

Thomadakis C. (2015) - The mechanisms of continuous tooth replacement in the Nile crocodile (*Crocodylus niloticus*) (PhD thesis). University of the Witwatersrand, 222 pp.

Vallcorba O., Canillas M., Audije-Gil J., Barroso-Barcenilla F., González-Martín A., Molera J., Rodríguez M.A. & Cambra-Moo O. (2021) - Synchrotron X-ray microdiffraction to study life history events in Cretaceous crocody-

lomorphs through dental structures. *Cretaceous Research*, 128: 104960.

Vallcorba O. & Rius J. (2019) - d2Dplot: 2D X-ray diffraction data processing and analysis for through-the-substrate microdiffraction. *Journal of Applied Crystallography*, 52(2): 478-484.

Westergaard B. & Ferguson M.W.J. (1986) - Development of the dentition in *Alligator mississippiensis*. Early embryonic development in the lower jaw. *Journal of Zoology*, 210(4): 575-597.

Westergaard B. & Ferguson M.W.J. (1987) - Development of the dentition in *Alligator mississippiensis*. Later development in the lower jaws of embryos, hatchlings and young juveniles. *Journal of Zoology*, 212(2): 191-222.